J. Fluid Mech. (1970), *vol.* 43, *part* 1, *pp.* 77–96
Printed in Great Britain

The three-dimensional mixing layer between two grazing perpendicular streams

By J. E. HACKETT† AND D. K. COX
Aerodynamics Division, National Physical Laboratory, Teddington, Middlesex

(Received 8 October 1969)

The three-dimensional mixing layer between two grazing perpendicular streams is investigated both theoretically and experimentally. Similar shear velocity profiles are present about 40 initial momentum thicknesses downstream of the splitter edges. Thereafter the velocity component in the resultant direction of the two streams is shown to be constant through the layer; the profile perpendicular to this (the shear direction) has approximately an error function form. The ratio of the maximum shear stress to the square of the shear velocity difference is about 50% greater than in a two-dimensional layer.

1. Introduction

There are numerous aerodynamic situations in which a turbulent shear layer exists between two streams whose directions are not the same. This occurs, for example, over the surface of a jet plume issuing from a surface into a mainstream, across a vortex sheet which is rolling up as from a slender delta at incidence and in most three-dimensional boundary-layer separations.

However, in many practical flows static pressure gradients and flow curvature complicate the mixing process and interpretation is difficult. Experiments have therefore been carried out in a plane layer between two horizontal uniform streams of the same velocity at right angles to one another and one above the other, which merge from each side of a 'splitter' edge.

Figure 1 is a perspective view of two contractions used in producing the mixing layer. One is above the other, and the centrelines are at right-angles. The thin splitter plate lies between the upper and lower streams which each have the same cross-sectional dimensions and speeds.

Downstream of the splitter there is an antisymmetric flow for which the only characteristic length dimension is in the x direction. The geometry gives velocity distributions which are antisymmetric in the direction parallel to the splitter (i.e. z) but symmetric in the x, y plane.

It is quite clear from experiments on 'simple' layers, between parallel streams, that the latter do not possess symmetries like this, even if a reference system is chosen which moves at the mean velocity of the two streams.

Figure 2 illustrates that the skewed layer is simpler than one involving parallel streams (including the single-stream case) because a set of particles contained

† Present address: Aerospace Laboratory, Lockheed-Georgia Company, Marietta, Georgia 30060, U.S.A.

in a plane normal to the splitter edge at time $t = 0$ occupies a mean position which is still planar after time Δt (see figure 2(*b*)). This cannot be said of flow in the 'single-sided' shear flow of figure 2(*a*). The present flow is thus one of quite fundamental importance.

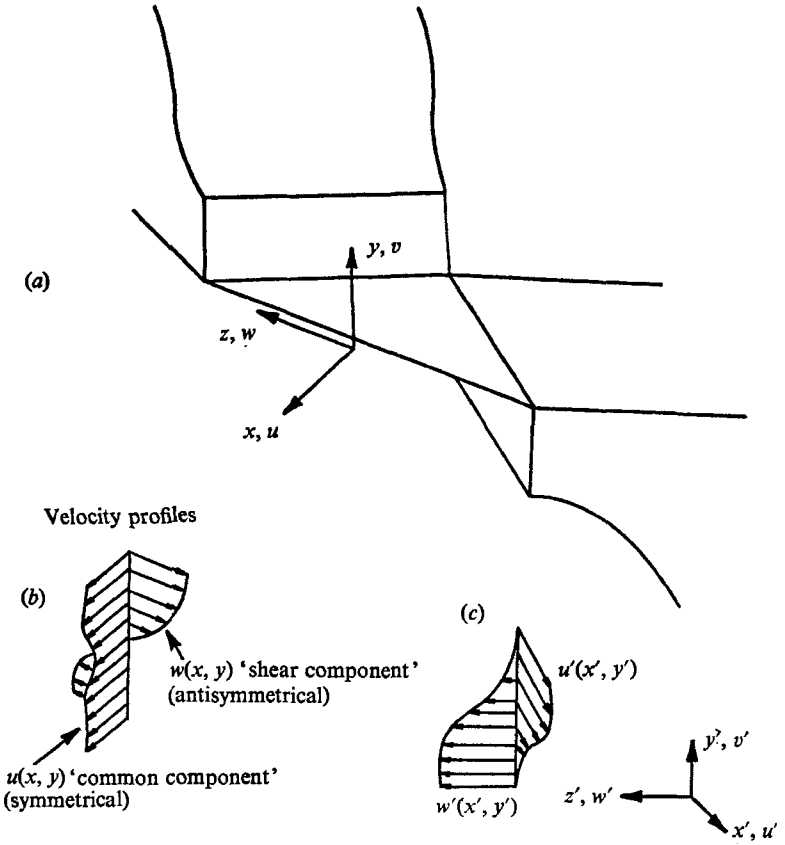

FIGURE 1. (*a*) The co-ordinate system. (*b*) and (*c*) Alternative projections of velocity profiles.

2. Analysis

We shall assume the spreading angle of the mixing layer is small, acknowledging that this is less well founded than for boundary layers, which spread more slowly. The appropriate axis system is in the common direction of the streams (x) and normal to the layer (y). Provided that disturbances do not propagate inwards from the ends of the splitter, there is no characteristic dimension in the z direction so that the equations of motion become:

$$u\frac{\partial u}{\partial x}+v\frac{\partial u}{\partial y}+\frac{\partial}{\partial x}(\overline{u'^2})+\frac{\partial}{\partial y}(\overline{u'v'}) = -\frac{1}{\rho}\frac{\partial p}{\partial x},$$

$$u\frac{\partial v}{\partial x}+v\frac{\partial v}{\partial y}+\frac{\partial}{\partial x}(\overline{u'v'})+\frac{\partial}{\partial y}(\overline{v'^2}) = -\frac{1}{\rho}\frac{\partial p}{\partial y},$$

$$u\frac{\partial w}{\partial x}+v\frac{\partial w}{\partial y}+\frac{\partial}{\partial x}(\overline{u'w'})+\frac{\partial}{\partial y}(\overline{v'w'}) = 0,$$

where ρ is the density and p the static pressure and here primes denote unsteady quantities.

Applying order arguments in which the thickness of the layer, δ, is assumed small relative to the distance from the origin, x, we see that derivatives with

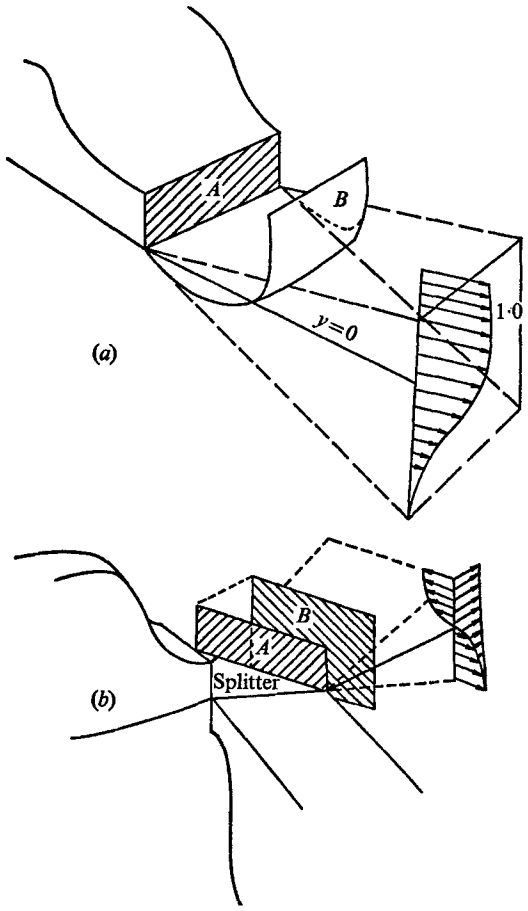

FIGURE 2. History of fluid particles in two- and three-dimensional shear layers. (*a*) Mixing layer between a single stream and ambient air. (*b*) The skewed mixing layer. *A*, position of a set of fluid particles at time 0; *B*, surfaces through the mean positions of the same fluid particles after time Δt.

respect to x will be δ times those taken with respect to y. Also, from the continuity equation, it is evident that $\partial v/\partial y = -\partial u/\partial x$ and hence v is δ times u in magnitude. It is also immediately obvious that u and w are each of the same order.

We next assume that, as is found experimentally in simpler turbulent mixing layers, products like $(\overline{u'w'})$ have the magnitude δ times (u^2). Taking $u\,\partial u/\partial x$ as $O(1)$ and noting that the relative magnitudes can be found by dividing throughout by $u\,\partial u/\partial x$ and then using the fact that y/x, v/u and $\overline{u'w'}/u^2$ are all $O(\delta)$, the equation of motion in the y direction becomes

$$O(\delta)+O(\delta)+O(\delta)+\frac{\partial}{\partial y}(\overline{v'^2}) = -\frac{1}{\rho}\frac{\partial p}{\partial y},$$

or

$$p+\rho\overline{v'^2} = f(x,z).$$

Since flow in each of the external streams is parallel and uniform, consideration of conditions at the edge of the layer gives

$$p+\rho\overline{v'^2} = p_\infty,$$

where p_∞ is the pressure at infinity and is constant. Thus

$$\frac{\partial p}{\partial x} = -\rho\frac{\partial}{\partial x}(\overline{v'^2}).$$

The equation of motion in the x direction is reduced to

$$u\frac{\partial u}{\partial x}+v\frac{\partial u}{\partial y}+\frac{\partial}{\partial x}(\overline{u'^2}-\overline{v'^2})+\frac{\partial}{\partial y}(\overline{u'v'}) = 0.$$

If, as is common in boundary-layer theory, we neglect $\partial(\overline{u'^2}-\overline{v'^2})/\partial x$ we have

$$u\frac{\partial u}{\partial x}+v\frac{\partial u}{\partial y}+\frac{\partial}{\partial y}(\overline{u'v'}) = 0. \tag{1}$$

The equation of motion in the z direction reduces to

$$u\frac{\partial w}{\partial x}+v\frac{\partial w}{\partial y}+\frac{\partial}{\partial y}(\overline{v'w'}) = 0. \tag{2}$$

The continuity equation is

$$\frac{\partial u}{\partial x}+\frac{\partial v}{\partial y} = 0, \tag{3}$$

and the boundary conditions are:

$$\begin{aligned} u(x,+\infty,z) &= u_0, & u(x,-\infty,z) &= u_0,\\ v(x,+\infty,z) &= 0, & v(x,-\infty,z) &= 0,\\ w(x,+\infty,z) &= -w_0, & w(x,-\infty,z) &= +w_0,\\ v(x,0,z) &= 0,\\ w(x,0,z) &= 0; \end{aligned}$$

also

$$\left(\frac{\partial u}{\partial y}\right)_{y=0} = 0, \quad \left(\frac{\partial w}{\partial y}\right) = 0$$

and

$$\left(\frac{\partial u}{\partial y}\right)_{y=\pm\infty} = \left(\frac{\partial v}{\partial y}\right)_{y=\pm\infty} = 0,$$

where $u_0 = w_0 =$ (mainstream speed)$/\sqrt{2}$.

We now attempt to solve equations (1), (2) and (3) for self-preserving flows.

Suppose that

$$\left.\begin{aligned} w &= w_0 f_1'(\eta),\\ u &= u_0 f_2'(\eta), \end{aligned}\right\} \tag{4}$$

and

$$\left.\begin{aligned} \overline{u'v'} &= u_0^2 h_{12}(\eta),\\ \overline{w'v'} &= w_0 u_0 h_{32}(\eta), \end{aligned}\right\} \tag{5}$$

where $\eta = y/x$.

Obviously u_0 and w_0 have associations with u' and w' and the continuity equation suggests that u_0, rather than w_0, should be associated with the v' components.

Using the derivative of (4), the continuity equation (3) becomes

$$u_0 \eta f_2''(\eta) - \partial v/\partial \eta = 0.$$

Therefore

$$v = u_0 \int_0^\eta \eta f_2''(\eta)\, d\eta$$

$$= u_0[\eta f_2'(\eta) - f_2(\eta) + f_2(0)].$$

Since $f_2(0)$ may be selected arbitrarily, we may place it equal to zero, giving

$$v = u_0[\eta f_2'(\eta) - f_2(\eta)]. \tag{6}$$

Substituting (4), (5) and (6) into (1) and (2), the equations of motion in the x and y directions become, respectively,

$$f_2 f_2'' - h_{12}' = 0 \tag{7}$$

(a solution of which is $f_2' = \text{constant}$, $h_{12}' = 0$) and

$$f_1'' f_2 - h_{32}' = 0. \tag{8}$$

To illustrate the suggested solution of equation (7), we next assume that the concept of eddy viscosity is valid in the present circumstances, namely

$$\overline{u'v'} = -\nu_{1T}(\partial u/\partial y).$$

This will be so if the flow is self-preserving, which is already implicit in the present analysis. Then we may write, on inserting $\partial u/\partial y$ from the definition in (4) and the definition of h_{12},

$$h_{12}(\eta) = -\frac{1}{R_2} f_2''(\eta), \tag{9}$$

where $R_2 = u_0 x/\nu_{1T}$.

Thus from equations (7) and (9)

$$f_2 f_2'' + \left(\frac{f_2''}{R_2}\right)' = 0.$$

The boundary conditions are

$$f_2'(+\infty) = f_2'(-\infty) = 1$$

and

$$f_2''(0) = 0.$$

One solution, and possibly the only one which satisfies the boundary conditions, is $f_2' = 1$. This holds even if $R_2 = R_2(\eta)$; i.e. if the eddy viscosity ν_{1T} varies through the layer, so long as R_2 remains finite. In this case

$$u = \text{constant} = u_0; \quad f_2 = \eta. \tag{10}$$

The solution of (8) may be obtained using a similar assumption with regard to eddy viscosity to that used above. However, here we put

$$\overline{w'v'} = -\nu_{3T}\partial w/\partial y.$$

Then we obtain

$$h_{32} = -\frac{1}{R_1} f_1'', \tag{11}$$

where $R_1 = u_0 x/\nu_{3T}$.

Substituting (10) into (8) gives

$$f_1'' \eta + \left(\frac{1}{R_1} f_1''\right)' = 0. \tag{11a}$$

Assuming R_1 = constant, the general solution to this equation is given by

$$f_1' = K_4 + K_3 \int_0^\eta e^{-\frac{1}{2}R_1\eta^2}\, d\eta.$$

Thus

$$w = w_0 \left(K_4 + K_3 \int_0^\eta e^{-\frac{1}{2}R_1\eta^2}\, d\eta \right). \tag{12}$$

Using the boundary conditions for w gives $K_3 = -1$ and $K_4 = 0$. Therefore

$$\frac{w}{w_0} = -\frac{2}{\pi^{\frac{1}{2}}} \int_0^\eta e^{-\frac{1}{2}R_1\eta^2}\, d\eta, \tag{13}$$

or

$$\frac{w}{w_0} = -\operatorname{erf}(\eta(\tfrac{1}{2}R_1)^{\frac{1}{2}}).$$

A more general result† may be obtained as follows. The general solution of (11a) is

$$f_1 = A \int_0^\eta R_1 \exp\left(-\int_0^\eta R_1 \eta\, d\eta \right) d\eta + B,$$

where A and B are integration constants. After evaluating A and B using the boundary conditions $f_1'(0) = 0$ and $f_1'(+\infty) = 1$ we obtain

$$f_1' = \frac{w}{w_0} = -\frac{\displaystyle\int_0^\eta R_1 \exp\left(-\int_0^\eta R_1 \eta\, d\eta \right) d\eta}{\displaystyle\int_0^\infty R_1 \exp\left(-\int_0^\eta R_1 \eta\, d\eta \right) d\eta},$$

which satisfies automatically the boundary condition $f_1'(-\infty) = +1$ and reduces to the expression (13) on putting R_1 = constant.

In calculating shear stress (τ_x and τ_y) from measured velocity profiles, we shall later require a further result, derived from (7) and (8). From (7)

$$\frac{1}{\rho u_0 w_0} \frac{\partial \tau_x}{\partial \eta} = h_{12}' = f_2 f_2'', \quad \text{where} \quad f_2' = f_2'(\eta) \equiv \frac{u}{u_0};$$

$$\frac{\tau_x}{\rho u_0 w_0} = \int f_2 f_2''\, d\eta = f_2 \int f_2''\, d\eta - \int (f_2')^2\, d\eta$$

$$= f_2' \int f_2'\, d\eta - \int (f_2')^2\, d\eta \tag{14}$$

† This was pointed out to us by Dr N. Hayasi.

upon changing the order of the product in the first term and rewriting it in terms of f_2. Similarly, from (8)

$$\frac{1}{\rho u_0 w_0}\frac{\partial \tau_y}{\partial \eta} = h'_{32} = f_2 f''_1 \quad \text{where} \quad f'_1 = f'_1(\eta) = \frac{w}{w_0},$$

$$\frac{\tau_y}{\rho u_0 w_0} = \int f_2 f''_1 \, d\eta = f'_1 \int f'_2 \, d\eta - \int f'_1 f'_2 \, d\eta. \tag{15}$$

Equations (14) and (15) may be evaluated from the experimental velocity profiles.

Equation (15) is not suitable for use with the single stream, even with axes rotated by 45°, owing to difficulties with the boundary conditions. The alternative, closely related, equation is given by Townsend (1956)

$$\frac{\overline{uv}}{u_0^2} = \int \eta \, d(f'^2_1) - f'_1 \int \eta \, d(f'_1) \tag{16}$$

on neglecting turbulent terms as before.

3. Apparatus, probes and experimental aspects

Figures 3 and 4 show the rig and test section layout. The requirement was for streams of not more than 150 ft./sec and Reynolds numbers of order 10^6 in the stream directions, so that equilibrium layers became well developed. Mixing-

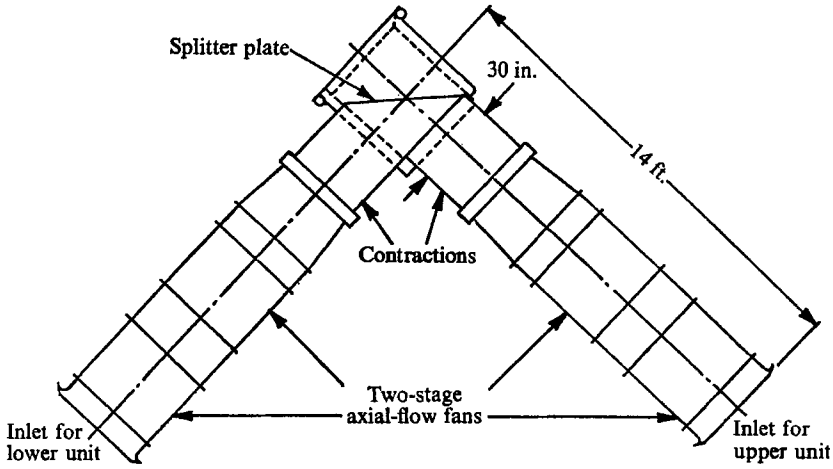

FIGURE 3. Plan view of the apparatus.

layer thicknesses were required which did not lead to small probe size and the associated difficulties with undue lags in pressure reading and in manufacture. It was also thought desirable to be able to set angles other than 90° between the streams, though in the event this ability was not exploited. However, it did make necessary two separate open return devices.

Axial flow fans and 'single-sided' contractions were used. A final contraction ratio of 4:1 and a stream breadth:height ratio of 4:1 were employed. The ranges

of commercially available axial fans were such that two-stage machines of 3 ft. diameter were the best proposition. The fan stages had common rotational sense and delivered approximately 14,000 cu.ft./min of air at 6 in. water pressure rise. A bleed at the base of the second stage motor fairing alleviated a central 'shadow' in total pressure at outlet and a peripheral bleed was used for fine adjustment when equalizing jet speeds. The speed of both streams was about 145 ft./sec at outlet, ordinary induction motors being used on the 50 c/s mains supply.

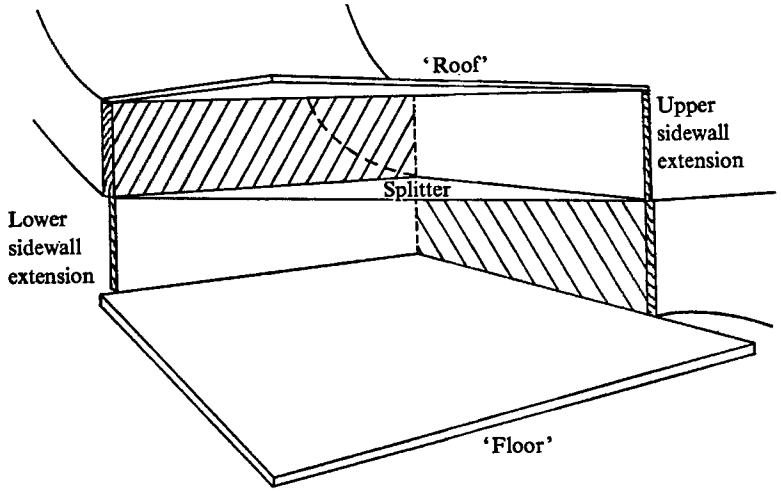

FIGURE 4. Perspective view of the apparatus, looking upstream in approximately the 'common' direction.

Further description of the rig and its design are given by Hackett & Cox (1967).

Figure 4 shows sidewall extensions to the contractions which prevented the development of mixing layers from the inner sides of the contractions. For obvious reasons, similar extensions from the outer sides of the contractions are undesirable and some loss of working area here had to be accepted. The triangular working area which resulted had a 42·42 in. base and a height of about 17 in.

It was a matter for conjecture whether or not a 'floor' and 'roof' should be fitted to the working area. However, had they not been fitted, double the thickness of mainstream would have been needed to prevent the top and bottom mixing layers meeting the experimental one, and the apparatus probably would have outgrown the room. It was appreciated that if the horizontal component of velocity normal to the splitter was affected by the shear parallel to it (and there was no reason to suppose it would not be), a displacement effect could arise leading to streamwise static pressure gradients in the mainstreams, dependent upon roof and floor constraint. As it was not possible to anticipate even the sense of such an effect, a horizontal roof and floor were fitted. This design was vindicated experimentally since the common component of velocity turned out to be approximately constant. The use of a Reynolds number normal to the splitter of about a million, which led to a bulky rig with quite high installed power, was

justified. With, say, half this value there would have been serious doubts as to whether self-preserving flow was fully established since virtual origins of mixing occurred several inches from the splitter under some conditions.

Experimental techniques

Flow direction, static and total pressures were measured at 'standard' positions shown in figure 5 using vertical traverses through the layer. The traverses at points along AB are intended for comparisons with theory while points along CD are more appropriate when comparing with single stream results, the upper

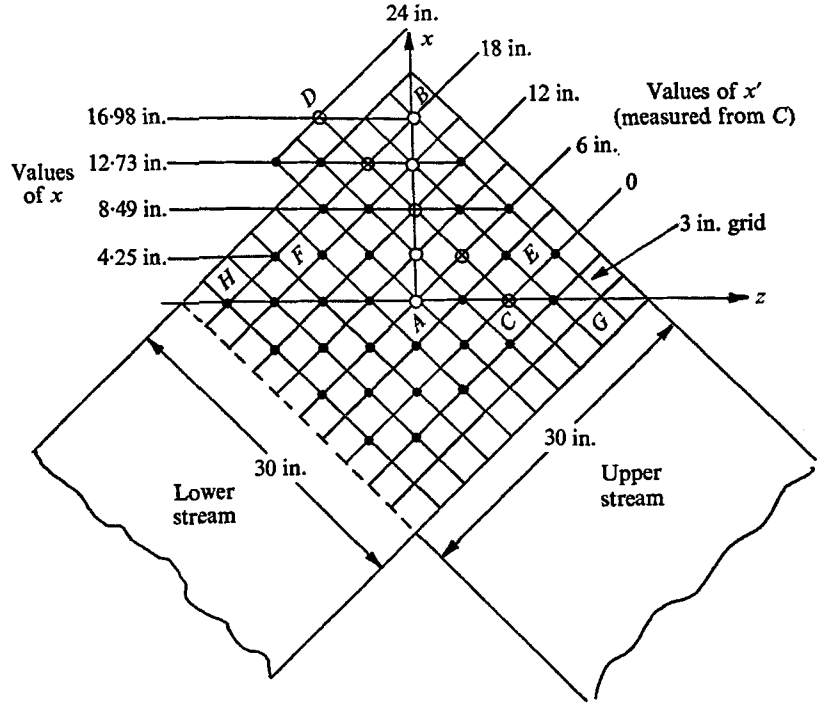

FIGURE 5. Traverse positions. ○, 'standard' positions (two stream runs); ⊗, 'standard' positions (single stream runs); ●, other available positions.

stream being used. The ninety degree range of yaw angle made it imperative to rotate probes about a vertical axis and initial measurements were always with a 5-hole instrument, shown in figure 6, nulled in yaw. Large vertical velocities were not expected so nulling was not attempted in pitch. However, upper minus lower tube differential pressure measurements were useful in setting up the apparatus, particularly in attaining correct antisymmetry, even though artificially high pitch indications were encountered in the shear layer.

In all traverses with the 5-hole instrument, five probe pressures, two reference pressure differences, yaw and vertical positions were measured using transducers and recorded upon punched tape prior to computer processing. Reference pressures were measured at points on the two contractions, centreline velocities used for normalization being determined using appropriate calibration constants.

Equalization of the speeds of the two streams was effected by equalizing total pressure readings at points 5 in. above and below the splitter for each particular traverse position.

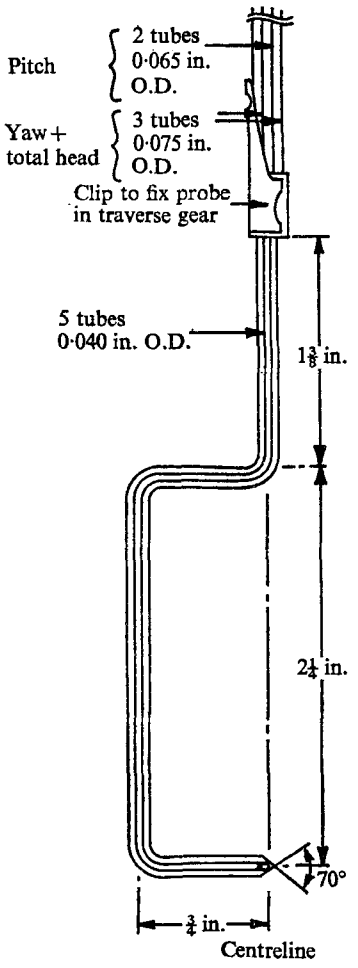

FIGURE 6. The 5-hole probe.

The mainstream flow quality was somewhat below wind tunnel standards, having a root-mean-square turbulence level of about 0·9 %, but this figure was still low in comparison with turbulence levels to be expected in the free shear layers. The turbulent boundary layers around the exits to the contractions were about ¼ in. thick and the measured growth along the roof and floor was equivalent to a displacement of about ¼°.

The attainment of appropriate initial conditions with both streams present was quite difficult. The symmetry of the whole flow was very sensitive to the ratio of upper to lower boundary-layer thickness, a situation aggravated in initial tests by the use of a boundary-layer controlled splitter, which tended to amplify this ratio. The more obvious indications of wrong initial conditions included the appearance, near the start of mixing, of symmetric components in the

indicated pitch distributions through the layer (which should be entirely anti-symmetric) and excursions in static pressure at the layer centre sometimes reaching several tenths of freestream dynamic pressure. However, once symmetries were correct, the fact that the boundary layers were turbulent at the start of

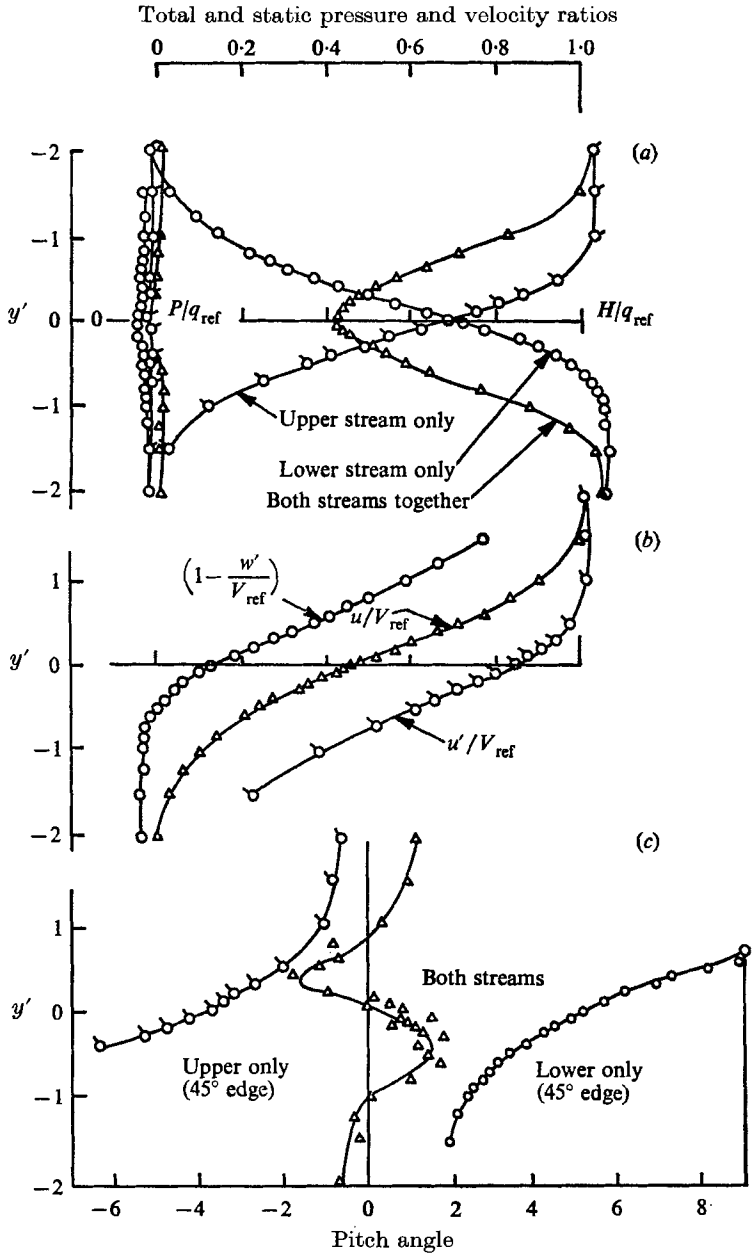

FIGURE 7. Typical flow measurements in two- and three-dimensional shear layers. $z = 0$, $x = 8{\cdot}6$ in. (i.e. $x' = 12{\cdot}1$ in.). (*a*) Total and static pressure ratios (upper scale). (*b*) Velocity ratios (upper scale). (*c*) Measured pitch angles (lower scale). [H is the total pressure, q is the dynamic pressure and V_{ref} is the freestream velocity.]

mixing delayed the approach to similarity less than the study by Bradshaw (1966) might suggest.

The typical results shown in figure 7 indicate that the 5-hole probe performance was quite good. Static pressure indications were fairly constant through both single-stream and skewed shear layers. The pitch velocity indications, though no more than 5 % of freestream, exceeded values to be expected from consideration of probe size and total pressure gradient; a fact also confirmed experimentally by using a half-scale probe. Since application of the continuity equation in the x, y plane for the skewed layer indicated vertical components of smaller magnitude, pitch indications were probably in error, possibly on account of large (turbulent) flow angles which exceeded the linear range of the probe. A more detailed discussion of 5-hole probe performance is given by Hackett & Cox (1967). Some of the tests which will be reported here were with the boundary-layer controlled splitter fitted, but with no suction applied. Other (later) tests were with $\frac{1}{8}$ in. thick metal splitter plate installed, chamfered at the trailing edge. This reduced the boundary-layer thickness at the start of mixing by about $\frac{1}{4}$ in. and reduced the maximum measured confluence angle in the vertical plane normal to the splitter from 8° to about $3\frac{1}{2}°$. (Boundary-layer control increased the maximum confluence angle.) The respective trailing edge angles were 3·8° and 2·6°.

Although the centre of the mixing layer lay in a horizontal plane with the boundary-layer control box fitted, it was swept downwards after fitting the thin splitter. A careful check of the geometry failed to explain this; the drift of the centre of the layer was downwards at about 1° in a plane normal to the splitter.

The displacement in figure 7 between the skewed-layer velocity profile and those for single layers is more marked than with the thin splitter fitted.

4. Experimental results

Comparison of two- and three-dimensional shear layers

As mentioned earlier, the skewed shear layer may be regarded either with respect to axes in one stream, for comparison with the more familiar two-dimensional layer, or relative to the axes used in the above analysis.

There are two apparent differences between the two- and three-dimensional situations. If we use, as a base line, results from the upper stream alone, with a shear layer starting from a normal edge, we must consider the effect of skewing this edge by 45° before examining the consequences of cross flow due to the addition of the lower stream.

In figures 8 and 9 we see that skewing the start of mixing by 45° has little effect on the two-dimensional shear layer though there may be a slight reduction in the spreading rate. However, as there was variation of boundary-layer thickness along the 45° edge, there was some doubt concerning the position of the virtual origin.

In the similar case of a boundary layer in zero pressure gradient starting at a swept leading edge, the results of Ashkenas (1958) show that the skin friction coefficient deduced from the logarithmic velocity profiles is unaltered by 45°

of sweep and therefore that the growth rate is unaltered; the direct measurements of growth rate show a small increase due to sweep. Some measurements by Carr-Hill (unpublished work at NPL) show a small increase in skin friction (5 % at 60° sweep). The final conclusion to be drawn is that turbulent shear flows are to a good approximation unaffected by slow spanwise changes (see also Bradshaw 1969).

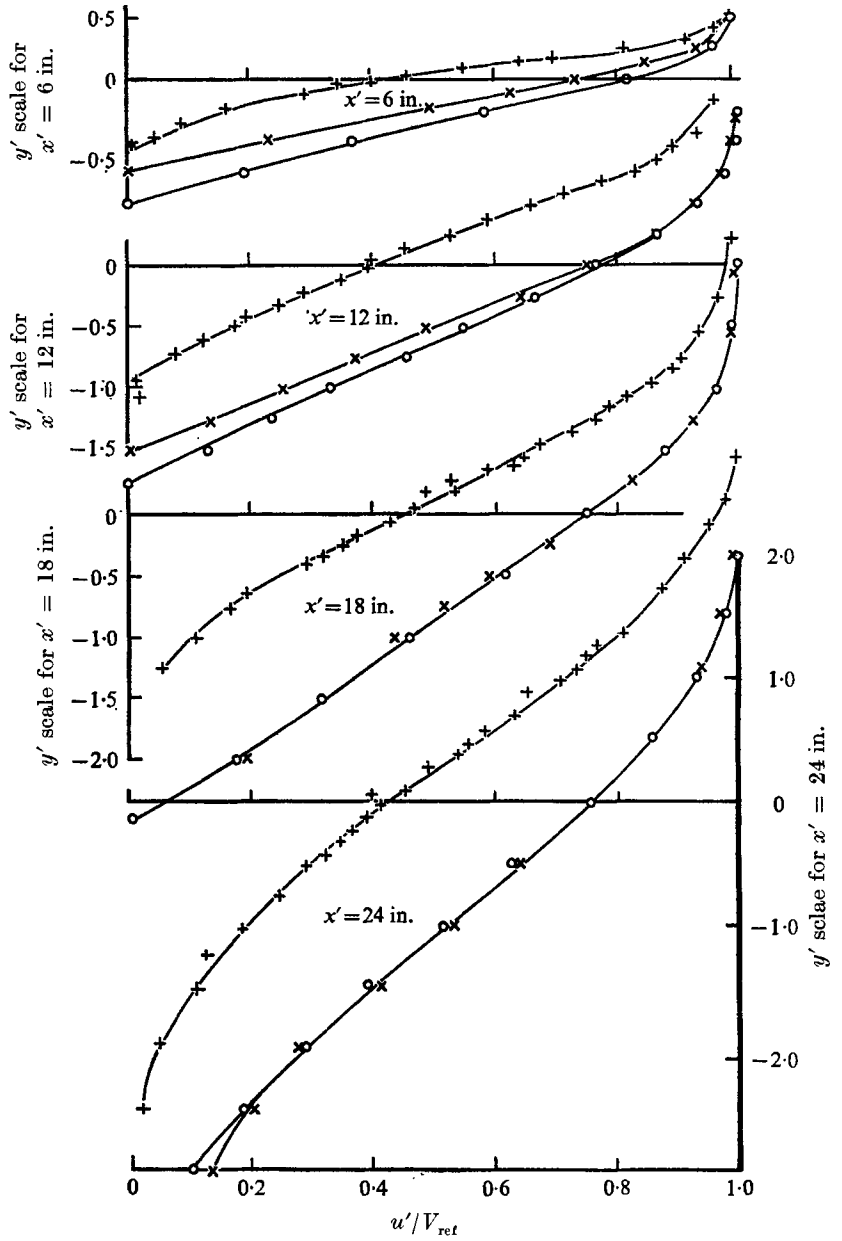

FIGURE 8. Velocity distributions for two-and three-dimensional shear layers. Thin splitter, ×, upper stream normal edge; ○, upper stream 45° edge; +, both streams based on $H^{\frac{1}{2}}$.

Upon adding cross flow we see an increase in velocity gradient in a direction normal to the upper stream (figure 8) accompanied both by a closing up of constant velocity rays (figure 9) and by a shift of the half-velocity line to a horizontal position. We may expect some similarity between the upper parts of the skewed-layer and the single-layer profiles, since there is little cross flow here, but at lower values of u, the cross flow is increasingly important and only if w is simply superposable may we expect any resemblance to the 'simple' case. To understand the skewed layer further, it is necessary to revert to axes normal and parallel to the splitter edge.

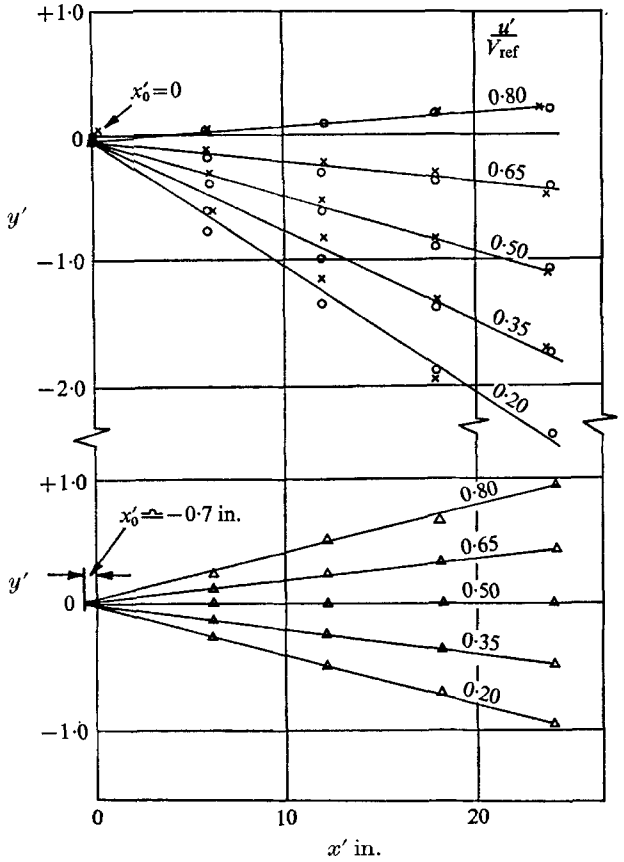

FIGURE 9. Spreading of two- and three-dimensional shear layers. ×, upper stream 90° edge; ○, upper stream 45° edge; △, both streams 45° edge.

Velocities in shear and common directions: comparison with theory

In figures 10 and 11 we see views of three-dimensional velocity profiles seen from above and looking outward from the splitter. The downward drift, mentioned previously, is evident in figure 11 but has been removed from later figures. Cross-plotting these figures gave straight rays (with a virtual origin, x_0 approximately 0·4 in. behind the splitter edge), thus justifying the similarity analysis above.

Another important feature is the constancy (to within $\pm 10\,\%$) of the common component. Although we see something like a wake development in u, the result

is in broad agreement with (10) and it seems reasonable to conclude that, had zero initial boundary layer been achieved by boundary-layer control, the common component would have been exactly constant, provided no stability problems arose in starting the mixing.

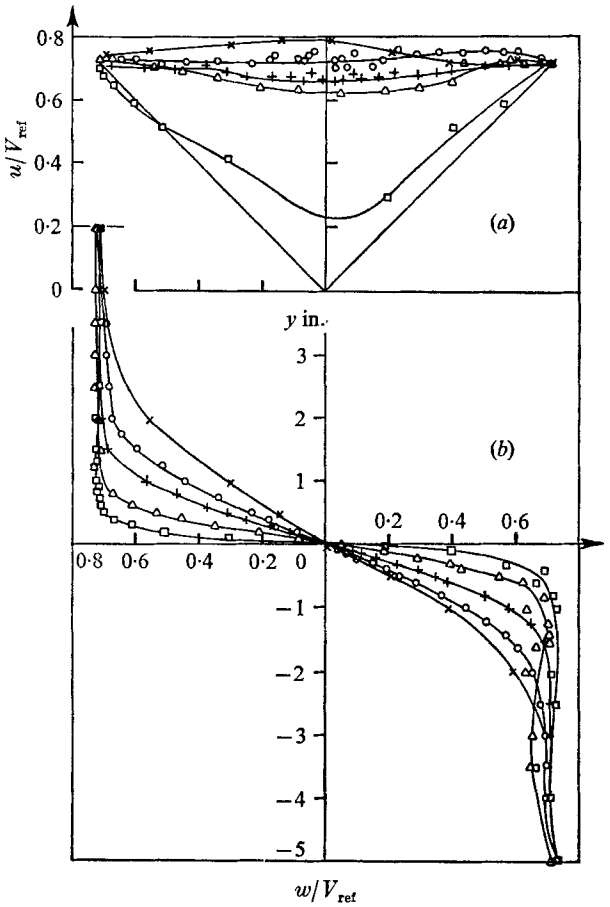

FIGURE 10. Velocity distributions in a skewed mixing layer. Boundary-layer control box fitted, but no suction applied. (*a*) Vector plot. (*b*) Shear velocity profiles. Values of x: □, 0·53 in.; △, 4·35 in.; +, 8·59 in.; ○, 12·90 in.; ×, 17·15 in.

In figure 12 the shear profiles (w) are plotted on a probability scale, upon which error functions such as equation (13) are straight lines. It is evident that the experimental results agree quite well with the predicted form. Eddy Reynolds numbers, derived from the slopes of the curves in figure 12, lay between 190 and 230, with no consistent variation with x. R_1 values were sensitive both to the choice of x_0 and to the choice of the best straight lines in figure 12.

Calculation of shear stresses

For comparisons between different shear flows it is simplest to consider a Reynolds number based on the shear velocity difference ΔU and a length scale typical of the local profile. If the length scale is $\delta_f = \Delta U/(\partial U/\partial y)_{\max}$, then the Reynolds

number $\Delta U\ \delta_f/\nu_T$ is equal to $\rho(\Delta U)^2/\tau_{\max}$, a simple measure of the turbulent intensity in the shear layer. Since the velocity profiles in jets, wakes and mixing layers are nearly similar, almost any length scale will do for comparisons between

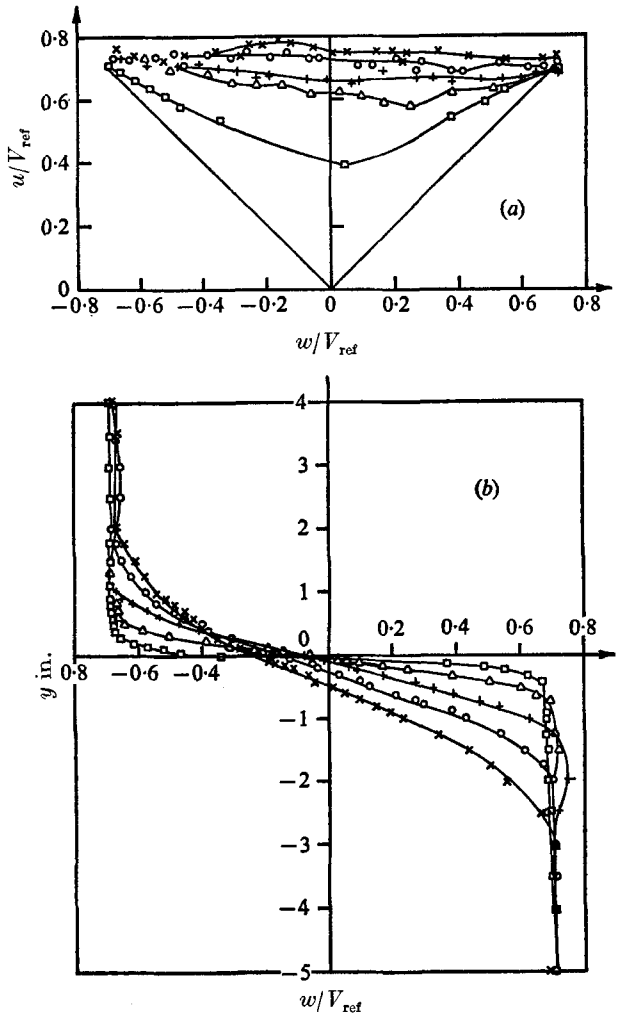

FIGURE 11. Velocity distributions in a skewed mixing layer. Thin splitter fitted. (*a*) Vector plot. (*b*) Shear profile. Value of x: □, 0·21 in.; △, 4·31 in.; +, 8·56 in.; ○, 12·80 in.; ×, 17·04 in.

different flows. It is difficult to measure δ_f accurately (one tends to take an average $\partial U/\partial y$ over a range of at least $0{\cdot}2\Delta U$ so that the resulting Reynolds number is $\rho(\Delta U)^2/\bar{\tau}$ where $\bar{\tau}$ is the average shear stress over the same range) and the best course is to derive $\tau_{\max}/(\Delta U)^2$ directly. In the present experiment τ has been calculated from the measured velocity profiles, using (15) and (16), a process that is not critically dependent on measurements of $\partial U/\partial y$.

The technique used for the two-dimensional layer was to curve fit the normalized experimental data at large scale and pick off η values for velocity ratios

of 1·00, 1·00, 0·99, 0·975, 0·95, 0·925, 0·900 and every 0·05 down to 0·10, 0·075, 0·050, 0·025, 0·000 and 0·000, plus a few extra near peak shear stress giving 33 points in total. The approach for the skewed layer was similar but involved a total of 37 points, the range $\pm 0{\cdot}7071$.

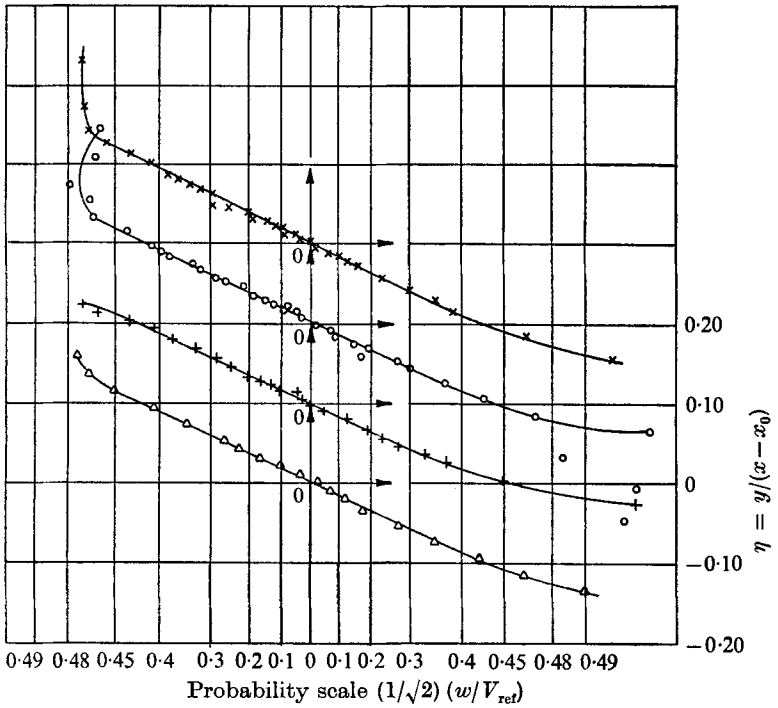

FIGURE 12. Probability plot of normalized shear velocities in a skewed shear layer. Thin splitter. Value of x: △, 4·31 in.; +, 8·56 in.; ○, 12·84 in.; ×, 17·24 in.

The determination of integration constants, by trial shifts in the value of zero offset in η to obtain equal results at the edges of the layer, was greatly aided by the use of a remote access computer terminal. The peak shear stress and the smooth blend to zero shear stress each required a detailed description of the profile at the ends of the velocity range. The single-stream calculation was more sensitive in this regard and differences between the present results and those we derived from the velocity profile given by Liepmann & Laufer (1947) may be due to difficulties of this sort. A deeper investigation of methods for applying (15) and (16) appears desirable.

Figure 13 shows shear stresses, τ_y, calculated as described above from experimental velocity profiles. The results for the skewed layer are for f_2' assumed to be unity; the inclusion of experimental f_2' variations produced a very similar result.

5. Discussion

The simplest way to think of the skewed mixing layer is as a mixing layer between two equal and opposite streams in the z direction, being translated bodily in the x direction (this is almost exactly the same as the unsteady mixing

layer between equal and opposite infinite streams impulsively started at $t = 0$, the resemblance being much closer than that between the boundary layer and the Rayleigh problem of the impulsively-started flat plate). We can then concentrate on the motion in the y, z plane, and compare the shear stress coefficient

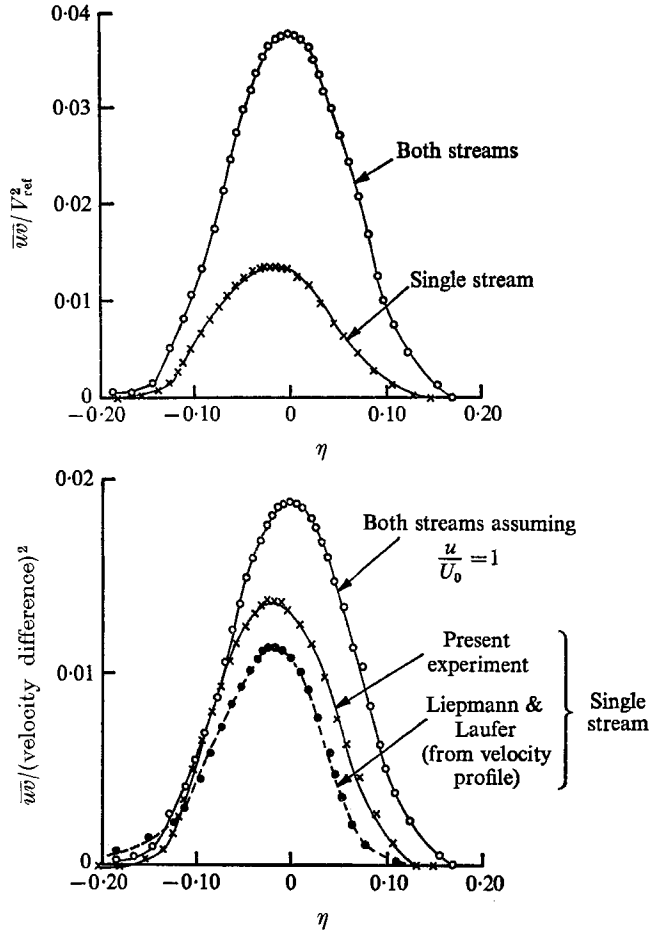

FIGURE 13. Shear stresses for two- and three-dimensional shear layers.

$-\overline{vw}/(2w_0)^2$ with $-\overline{uv}/U_1^2$ or, in general, $\overline{uv}/(\Delta U)^2$. Since all free shear layer velocity profiles are nearly similar, the shear stress profiles are nearly similar and we need compare only $\overline{uv}_{max}/(\Delta U)^2$, which was shown above to be the reciprocal of a conveniently-defined eddy Reynolds number. Values of $\overline{uv}_{max}/(\Delta U)^2$ in different flows are:

Single mixing layer	1/110
Liepmann & Laufer (1947) (present calculation from velocity profile)	1/87·5
Present experiment, single mixing layer	1/72·5
Skewed mixing layer	1/53·2
Two-dimensional jet (Bradbury 1965)	1/42
Wake (Townsend 1956)	1/30

The major difference between the two types of mixing layer is evidently not the three-dimensionality as such, which reduces to the addition of a uniform translation (figure 2), but the absence of v component mean velocity in the case of the skewed mixing layer. Townsend (1956) has suggested that the presence of appreciable negative $\partial V/\partial y$ in jets is largely responsible for the difference in eddy Reynolds number between jets and wakes, because of the consequent restraint on growth of the large eddies, and Gartshore (1965) has produced a simple analysis for self-preserving flows which, with an empirical constant, gives

$$\frac{1}{R} = \frac{1}{R_0}\left(1 + 10\frac{\partial V/\partial y}{\partial U/\partial y}\right)$$

and reconciles jet and wake measurements very well. In the region of maximum $\partial U/\partial y$ in a single mixing layer, $(\partial V/\partial y)/(\partial U/\partial y)$, which is just $-y/x$, is of the order of 0·03, so that Gartshore's formula suggests that the ratio of shear-stress coefficients in the skewed and single layers should be roughly 1·4, other things being equal. Since the ratio determined experimentally was 72·5/53·2, or 1·36, almost all of the difference between the two types of mixing layer may be attributed to the difference in v component behaviour.

Since the variations in common-component velocity seem to be attributable to the initial boundary layer and would not occur in the ideal mixing layer, it is not realistic to calculate the common component of shear stress; it would undoubtedly be very small. Therefore we may say that in the ideal layer the shear stress would have the same direction as the velocity gradient; the experiment throws no light on whether this would be the case in a general three-dimensional flow in which the direction of the resultant velocity gradient varied from point to point.

6. Conclusions

A skewed mixing layer (figure 1) has been investigated both theoretically and experimentally. It may be thought of either as a mixing layer between equal and opposite streams in the z direction which is translated bodily in the x direction, or as a simple shear layer from a 45° edge subjected to a cross-flow. Whichever view is taken, symmetry demands that there can be no mean vertical velocity at the centre of the layer, which contrasts with the single-stream shear layer.

Similar shear velocity profiles were evident approximately 4 in. downstream of the splitter edges; i.e. about 40 times the upper-plus-lower boundary layer momentum thickness at the start of mixing. The 'common' component of velocity u (figure 1) tended to a constant value thereafter, giving zero mean vertical velocity in the layer and zero displacement thickness. This is the form predicted by equation (10) of the analysis and is of some importance in the rolling-up of vortex sheets, of which the present layer is an idealization.

The constancy of the u component, combined with an eddy viscosity assumption, leads to an error function form for the 'shear' component of velocity, w. This has been confirmed experimentally. The value of local eddy Reynolds number, based on the thickness over which the central 50 % of shear velocity difference

occurs, lay between 18 and 22. The dimensionless eddy viscosity, using velocity gradient at $y = 0$, was 1/42.

The ratio of maximum shear stress to the square of velocity difference, derived from shear velocity profiles, is approximately 1·4 times larger than in a simple mixing layer, at least very probably because of the absence of streamline convergence in the x, y plane, whose effect is predicted by Gartshore (1965).

The above comments apply only to cases of self-preserving three-dimensional shear flows in which curvature and pressure gradient are small.

Experiments on the layer between a single stream and ambient air showed little change on proving the starting edge from a normal to a 45° position. It is pointed out that the results of Ashkenas (1958), properly interpreted, lead to the same conclusions for the boundary layer.

The authors are indebted to many members of the N.P.L. Aerodynamics Department workshop staff who took part in the construction and day-to-day maintenance of the apparatus, and to Mr R. F. Johnson who was responsible for the efficient operation of the data logging equipment. We are particularly grateful to Mr P. Bradshaw for constructive comments throughout and his considerable help in tidying up loose ends after the senior author's departure. Thanks are also due to Mr N. Gregory for comments at the draft stage and to Professor J. T. Stuart for help with the mathematics.

REFERENCES

Ashkenas, H. L. 1958 *NACA TN* 4140.

Bradbury, L. J. S. 1965 *J. Fluid Mech.* **23**, 31.

Bradshaw, P. 1966 *J. Fluid Mech.* **26**, 225–236.

Bradshaw, P. 1969 *N.P.L. Aero Rep.* 1286.

Gartshore, I. 1965 Ph.D. Thesis, University of Cambridge.

Hackett, J. E. & Cox, D. K. 1967 *N.P.L. Aero Rep.* 1248.

Liepmann, H. W. & Laufer, J. 1947 *NACA TN* 1257.

Townsend, A. A. 1956 *The Structure of Turbulent Shear Flow.* Cambridge University Press.